and data transfer channels of the sections are combined in the switching module of the string, which is connected with the central control unit of a cluster.

The basic configuration of each of the 12 clusters in the NT-1000 neutrino telescope contains eight strings, each including 24 optical modules (two sections in a string) separated from each other by 60 m. The distance between adjacent clusters reaches 300 m. The string clusters are connected with the shore center by combined electrooptical cables about 6 km in length. Each cluster of the NT-1000 telescope is a functionally complete detector (with the detection volume on the scale of NT-200+ or ANTARES detector), which can operate both incorporated into the setup and independently. This provides the simplicity of expanding up the telescope instrumented volume and the possibility of bringing into operation its separate parts during the deployment of NT-1000.

The basic configuration of the telescope provides an efficient volume of 0.2–0.7 km^3 for recording showers in the energy range from 10^5 to 10^9 GeV, and an efficient area of 0.2–0.5 km^2 for recording muons in the energy range from 10^4 to 10^6 GeV. The accuracy of recovering the muon propagation direction ranges $0.4° - 0.6°$, and that for showers is $5° - 7°$. The relative accuracy of the shower energy recovery comes to 20–35%.

Long-term full-scale tests of the equipment of the NT-1000 section were successfully performed in Lake Baikal between 2008 and 2010. A prototype of the NT-1000 cluster was already constructed and tested under laboratory conditions and will be deployed in Lake Baikal in the continuous data acquisition regime during the winter expedition in 2011.

4. Conclusions

Thus, the method of deep-sea recording of elementary particles (and its ice modification) proved its efficiency for studying natural high-energy neutrino fluxes. The modern knowledge of the diffusion neutrino flux in the energy range from 10^{13} to 10^{18} eV, local sources of neutrinos with energies above 10 GeV, the natural flux of fast magnetic monopoles, and dark matter massive particles manifestations is mainly determined by the results of experimental studies performed with the Baikal NT-200/NT-200+ neutrino telescope, the AMANDA detector at the South Pole, and (in late 2009 and 2010) the ANTARES detector in the Mediterranean Sea. Bringing the IceCube detector into operation at the South Pole will provide the increase in the sensitivity of some experimental studies by one–two orders of magnitude.

On the agenda is the problem of the construction of a detector (or detectors) in the North Hemisphere for studying the center of our Galaxy with a sensitivity comparable to that of the IceCube detector. The Baikal collaboration, which developed, constructed, and prepared for full-scale tests a prototype of the basic element — an autonomous cluster of deep-sea strings of recording modules for the km3-scale NT-1000 detector (Baikal-GVD) — is considerably ahead of all on the part to constructing the operating project of such a detector.

References

1. Markov M A, in *Proc. of the 1960 Annu. Intern. Conf. on High-Energy Physics, Rochester, New York, 25 August – 1 September 1960* (Eds J Prentki, J Steinberger) (Rochester, N.Y.: Univ. of Rochester, 1960) p. 572
2. Baikal Collab. "Nauchno-tekhnicheskii proekt glubokovodnogo neitrinnogo teleskopa kubokilometrovogo masshtaba na oz. Baikal" ("Scientific and technical project of the km^3-scale neutrino telescope in the Lake Baikal"), http://baikalweb.jinr.ru/GVD/ (2010)
3. Katz U F (for the KM3NeT Consortium) *Nucl. Instrum. Meth. Phys. Res. A* **602** 40 (2009)
4. Circella M (for the ANTARES Collab.) *Nucl. Instrum. Meth. Phys. Res. A* **602** 1 (2009)
5. Andres E et al. *Astropart. Phys.* **13** 1 (2000)
6. Abbasi R et al. (and the IceCube Collab.) *Nucl. Instrum. Meth. Phys. Res. A* **601** 294 (2009)
7. Bagduev R I et al. *Nucl. Instrum. Meth. Phys. Res. A* **420** 138 (1999)
8. Baikal Collab. "The Baikal neutrino telescope NT-200", Preprint No. 92-03 (Moscow: INR RAS, 1992)
9. Avrorin A V et al., Preprint No. 1265/2010 (Moscow: INR RAS, 2010)
10. Balkanov V A et al. *Yad. Fiz.* **62** 1015 (1999) [*Phys. At. Nucl.* **62** 949 (1999)]
11. Balkanov V A et al. *Astropart. Phys.* **14** 61 (2000)
12. Aynutdinov V et al. *Astropart. Phys.* **29** 366 (2008)
13. Antipin K et al. *Proc. of the First Workshop on Exotic Physics with Neutrino Telescopes: EPNT'06, Uppsala, Sweden, September 20 – 22, 2006* (Ed. C P de los Heros) (Uppsala: Uppsala Univ., 2007)
14. Avrorin A et al., in *Proc. of the 31st ICRC, Lodz, Poland, July 2009*; arXiv:0909.5589
15. Avrorin A V et al., Preprint No. 1211/2009 (Moscow: INR RAS, 2009)]
16. Avrorin A V et al. *Pis'ma Astron. Zh.* **35** 723 (2009) [*Astron. Lett.* **35** 651 (2009)]
17. Aynutdinov V *Astropart. Phys.* **25** 140 (2006)

# Telescope Array Observatory observations of the Greisen–Zatsepin–Kuzmin effect

I I Tkachev

1. Introduction

The enigma of the origin of ultrahigh-energy cosmic rays (UHECRs) is one of the most interesting and important unsolved problems of particle astrophysics. The center of attention in this research field is the Greisen–Zatsepin–Kuzmin (GZK) effect. Recently, the Telescope Array (TA) observatory, the largest observatory in the northern hemisphere of Earth, studying the origin of UHECRs, began to operate in the state of Utah (USA). In this report, we consider the fundamentals of the GZK effect, its history and present observational status, and preliminary results obtained at the

I I Tkachev Institute for Nuclear Research,
Russian Academy of Sciences, Russian Federation
E-mail: tkachev@ms12.inr.ac.ru
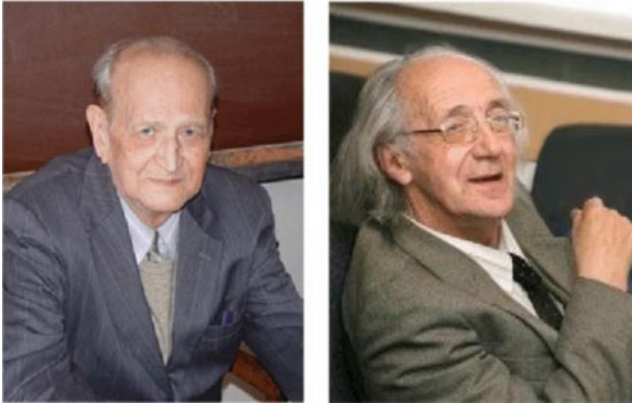
G T Zatsepin (at the left) and V A Kuzmin became staff members of INR, RAS from the first days of its foundation.

TA observatory, including the energy spectrum, composition, and the results of investigations of the arrival directions of initial UHECR particles.

Soon after the discovery of the cosmic microwave background (CMB) radiation of the Universe, Greisen [1], and Zatsepin and Kuzmin [2] pointed out that highest-energy protons propagating over cosmological distances from a source to an observer should catastrophically loose their energy in the threshold reactions of the photoproduction of pions in interactions with the universal background radiation. This process considerably limits the possible distance to the sources of detected UHECRs, which, according to the GZK limit, cannot exceed 100 Mpc, and should lead to the cutoff of the high-energy part of the spectrum.

The discovery made by Greisen, Zatsepin, and Kuzmin is based on physical observations and laws, which were well investigated and verified under laboratory conditions, in particular, on the cross sections for interactions between particles measured for energies of order 1 GeV (in the center-of-mass system) and on the validity of the general relativity theory and Lorentz's transformations. Thus, the question of whether the GZK flux suppression exists in the observed spectrum of cosmic rays is one of a number of fundamental questions because the absence of such a cutoff in the spectrum would be an unambiguous signal of 'new physics'.

On the other hand, the observational verification of the GZK cutoff of the high-energy part of the spectrum would suggest that the optical thickness of the cosmic medium for initial high-energy particles becomes comparable to a scale at which the Universe is noticeably inhomogeneous because the distribution of matter is inhomogeneous on scales of a few hundred megaparsec (and smaller). This means that the anisotropy of the UHECR flux can be anticipated in this case. It should be emphasized here that it is not only variations of the flux on large angular scales that are expected. It is also possible that we are standing at the threshold of discovering UHECR point sources. The astronomy of charged particles originating before our eyes may have a bright future if a noticeable fraction of initial particles consists of protons. This means that the study of the mass composition of initial UHECR particles is very important.

It is no wonder that great efforts in recent decades have gone into careful measurements of the spectrum of ultrahigh-energy cosmic rays, while the GZK effect is a source of growing interest in investigations conducted in the field of cosmic ray physics.

2. Effects of propagation of ultrahigh-energy cosmic rays

In this section, we consider the influence of different cosmological factors on the propagation of UHECRs and manifestations of this influence in observational data.

2.1 The Greisen–Zatsepin–Kuzmin cutoff

2.1.1 Optical depth. Ultrahigh-energy cosmic rays do not freely propagate in space and on cosmological scales. Their energy is sufficient for producing massive secondary particles in collisions with relic photons and also, depending on the nature of an initial particle, with radio photons and infrared photons.

The most important reaction is the photoproduction of pions during the propagation of protons (or neutrons) in the cosmic microwave background radiation left over from the hot Universe epoch. The threshold energy of this reaction in the laboratory reference system is defined as

$$E_{th}(p + \gamma \rightarrow n + \pi) = \frac{(m_p + m_\pi)^2 - m_p^2}{2E_\gamma(1 - \cos\theta)} . \tag{1}$$

It should be noted that this expression was derived using standard Lorentz transformations and standard dispersion relations $E^2 = k^2 + m^2$ between the energy and momentum of particles. If these assumptions are incorrect in the ultrahigh-energy region, the threshold conditions in the laboratory coordinate system can be different. For the black-body spectral distribution of relic photons at the temperature $T = 2.7$ K, reaction (1) becomes efficient for

$$E_{GZK} \gtrsim 5 \times 10^{19} \text{ eV} . \tag{2}$$

The pion photoproduction reaction has a large cross section and reaches a maximum at the Δ resonance. At the resonance half-width, this cross section equals

$$\sigma \sim 300 \text{ μb} \approx 3 \times 10^{-28} \text{ cm}^2 . \tag{3}$$

The number density of relic photons is $n \sim T^3 \sim 400$ cm^{-3}. This corresponds to the proton mean free path

$$L_\sigma = (\sigma n)^{-1} \approx 8 \times 10^{24} \text{ cm} \approx 2.7 \text{ Mpc}. \tag{4}$$

In each collision, an initial proton loses about 20% of its energy (corresponding to the pion–proton mass ratio). The proton energy decreases exponentially (by a factor of e) in a series of successive collisions after propagation over the distance L_A, called the decay length. For energies exceeding the resonance energy $E \approx 5 \times 10^{20}$ eV, the decay length is $L_A \approx 10$ Mpc. Thus, energy decreases to values close to the threshold at 10^{20} eV after propagation over distances of order 100 Mpc, virtually independently of the initial energy (Fig. 1).

Thus, *protons detected with energies $E \gtrsim 10^{20}$ eV should be accelerated in sources located at the distance $R \lesssim R_{GZK}$*, $R_{GZK} \equiv 100$ Mpc. The corresponding spatial volume is called the GZK sphere (or the GZK distance).

2.1.2 Spectral cutoff. We assume that the injection spectrum for initial photons exhibits a power form, $J_{in}(E) \propto E^{-\alpha}$, and $n(r)$ is the density of sources. The particle flux from an individual source decreases as r^{-2}, which is compensated for by the integration volume $r^2 \, dr$. Therefore, the cosmic ray
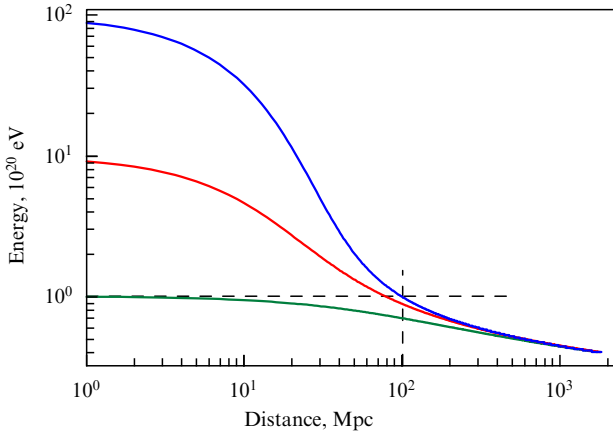
Figure 1. Initial proton energy as a function of the distance travelled from a source.

flux with energy E should increase proportionally to the radius of the integration sphere:

$$J(E) \propto \int_0^{R(E)} n(r)\, \mathrm{d}r \propto R(E)\,, \qquad (5)$$

if the density of sources remains invariable. Here, $R(E)$ corresponds to the decay length, i.e., the maximum distance to the sources of initial particles detected with energy E. The decay length for protons with energies $E < 5 \times 10^{19}$ eV is 10^3 Mpc, whereas for $E > 5 \times 10^{20}$ eV, the decay length is 10 Mpc.

Thus, *the UHECR flux should change by two orders of magnitude at the GZK energy if the distribution of sources is homogeneous* (Fig. 2).

2.2 Magnetic fields

Let us estimate a typical angle $\sim L/R_{\mathrm{g}}$ through which the trajectories of charged particles deflect after passing over the distance L in galactic and intergalactic magnetic fields. Here, R_{g} is the Larmor radius, and the angle of deflection is assumed small.

(1) For particles intersecting a galactic disc transversely to a galactic magnetic field, we have

$$\frac{\Delta\theta}{Z} \approx 2.5^\circ \, \frac{10^{20}\,\mathrm{eV}}{E} \, \frac{B}{3\,\mu\mathrm{G}} \, \frac{L}{1.5\,\mathrm{kpc}}\,, \qquad (6)$$

where Z is the electric charge of the initial particle, $3\ \mu$G is the value of the regular component of the magnetic field, and 1.5 kpc is the galactic disc thickness. (The weaker deflections in the turbulent component of the galactic magnetic field are discussed, for example, in paper [3].) Protons with energies $E > 10^{18}$ eV intersect the galactic disc during one passage. The trajectories of protons with lower energies 'become entangled' and escape from the Galaxy, diffusing through its boundary.

Cosmic rays with energies $E > 10^{18}$ eV should have an intergalactic origin if the initial particles comprise protons. Even if the UHECR composition corresponds to iron nuclei, cosmic rays for $E > 2 \times 10^{19}$ eV should enter the Galaxy from outside, otherwise the anisotropy of a particle flux on the galactic disc should be observed, which is not the case.

(2) The deflection angle of UHECR trajectories in a homogeneous random intergalactic field with the coherence
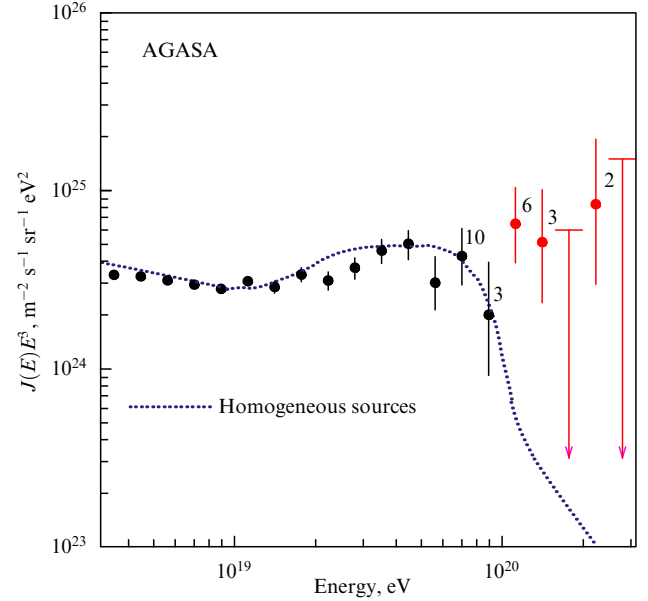
Figure 2. Energy spectrum of cosmic rays. The dotted curve fits the GZK expectation; dots show AGASA data (Akeno Giant Air Shower Array); numbers alongside the dots indicate the number of detected events (current data are discussed in Section 3).

length λ is determined by the relation

$$\frac{\Delta\theta}{Z} < 0.4^\circ \, \frac{10^{20}\,\mathrm{eV}}{E} \, \frac{B}{10^{-10}\,\mathrm{G}} \, \frac{(L\lambda)^{1/2}}{10\,\mathrm{Mpc}}\,. \qquad (7)$$

Intergalactic magnetic fields have not been measured to date, except for the central regions of galactic clusters. The observational restrictions on their value and correlation length are presented in Ref. [4]. The numerical simulation of the magnetic field generation processes in galactic clusters gives the upper theoretical limit for inductions of these fields on the order of $B \lesssim 10^{-12}$ G [5]. The lower limit of $B \gtrsim 3 \times 10^{-16}$ G was recently obtained in Ref. [6]. This limit follows from the fact of nonobservation of secondary gamma radiation from electromagnetic cascades induced by initial TeV photons.

Because the sources of highest-energy cosmic rays should be located inside the GZK sphere, the trajectories of protons with $E > 10^{20}$ eV are not deflected considerably by galactic or intergalactic magnetic fields, the deflections being comparable with the angular resolution of modern telescopes.

Thus, *the arrival directions of initial protons with energies exceeding the GZK energy should indicate their sources. The astronomy of charged particles is principally practicable.*

3. Observational status

For particle energies below 10^{14} eV, the cosmic ray flux is intense enough, so that direct observations are possible with the use of high-altitude balloons or satellites. For an energy of 10^{15} eV, the flux is one particle per 1 m² over a year, which excludes the possibility of direct orbital observations. For an energy of 10^{20} eV (the energy region where the GZK flux suppression should be manifested), the flux decreases to one particle per km² over a century, which, notably, is a reason for the slow progress in UHECR physics. However, difficulties involved in the direct observation of UHECRs would be

caused not only by their negligibly small flux but also by the extremely high energy being measured (recall that detectors of modern colliders weigh a few hundred thousand tons).

Fortunately for physicists working in this field, most of the detector has already been created by Nature — Earth's atmosphere being a suitable calorimeter. The atmosphere thickness is such that extended air showers (EASs), consisting of secondary particles induced by the incident initial particle, reach a maximum near Earth's surface. For an energy of 10^{19} eV, the transverse size of the air shower on the Earth surface achieves a few kilometers.

Thus, air showers can be detected by placing an array of particle detectors on Earth's surface, typically separated by a distance of a few hundred meters. Such a setup will accumulate data continuously. Other methods for detecting EASs are also possible, for example, based on the measurement of the fluorescence of the atmosphere caused by the passage of EASs. Such detectors can accumulate data only during clear, moonless nights. However, their advantages include the possibility of direct observations of important parameters, such as the longitudinal profile of a shower and the atmospheric altitude at which this profile reaches its maximum and the possibility of using the calorimetric method to estimate the energy of the initial particle.

In early experiments in the GZK energy region, such as Volcano Ranch [7], SUGAR (Sydney University Giant Air Shower Recorder) [8], Haverah Park [9], Yakutsk [10, 11], and AGASA [12, 13], the first method for detecting EASs based on detector arrays was utilized. Later on, the Fly's Eye [14] and HiRes [15] 'telescopes' appeared, which measured the fluorescent glow of the atmosphere. The results of earlier experiments were impressive but contradictory, and required verification and confirmation. It became clear that hybrid setups are required which use simultaneously a surface detector array and fluorescence telescopes for detecting the same EASs. Such a hybrid approach, which allows the reduction of systematic errors and determining more accurately the physical characteristics of the initial particle, because many EAS parameters are measured simultaneously, was applied to the development of the newest generation of observatories detecting cosmic rays, such as the Pierre Auger Observatory in the southern hemisphere of Earth [16], and the Telescope Array in the northern hemisphere [17].

3.1 Early results and theorists' growing interest in the GZK problem

To emphasize the importance of the discovery of Greisen, Zatsepin, and Kuzmin, we present here the historical review of early experimental results and describe briefly the considerable excitement generated by these results among theorists in the field of high-energy and particle physics.

Over four decades after the publication of papers by Greisen, Zatsepin, and Kuzmin [1, 2], the number of events detected with energies exceeding the GZK limit increased; however, no signs of the spectral cutoff or indications of possible particle sources were found. In particular, the spectrum measured with AGASA, the largest facility for recording EASs and which accumulated the most complete statistics by the time of the appearance of the last generation of observatories, is illustrated in Fig. 1.

These experimental results proved to be a puzzle because, unlike expectations based on the Standard Model, it was found that:

— the GZK cutoff was absent in the UHECR spectrum. Notice that the assumption that initial particles consist of heavy nuclei or photons does not solve this problem, and

— the arrival directions of particles with energies $E \gtrsim 10^{20}$ eV do not lead to the identification of astrophysical sources inside the GZK sphere.

This attracted interest and attention to this problem, and theorists proposed many possible solutions to this puzzle. Consider below some of them.

● *Invisible sources.* To explain the second part of the puzzle related to the arrival directions of initial particles, a hypothesis was advanced that the UHECR sources are not unique, bright astrophysical objects, which usually attract attention, but *something* that was located (or is located) inside the GZK sphere, but is invisible today and does not reveal itself as a source, except for the presence of luminosity in UHECRs. As objects of this type, 'dead' quasars were proposed [18]. The model assumes that quasars, which were bright and powerful in the past, preserve their capability to accelerate protons near the horizon of a supermassive black hole, even when the matter accretion process has terminated and the quasar is quenched in the electromagnetic spectral range. However, this model is intrinsically contradictory. The acceleration of protons up to ultrahigh energies in such a compact object is inevitably accompanied by intense gamma radiation in the TeV-energy range, and more recent results obtained with Cherenkov gamma telescopes exclude this model [19].

● *'Local' models.* The GZK cutoff will be absent in the UHECR spectrum if the sources of cosmic rays are located in the galactic halo. Such a scenario is implemented in the hypothesis of decomposing superheavy dark matter [20, 21]. The problem of generating superheavy, but long-lived (and, therefore, noninteracting) particles is solved quite simply. Dark matter particles in the required mass range $M_X \sim 10^{13}$ GeV are created at the right cosmological concentration due to the Universe expansion process itself [22–24]. The model of decomposing superheavy dark matter has an unambiguous signature: the anisotropy of the UHECR flux at the galactic center [25, 26]. This characteristic is not observed in real data.

● *Models with 'intermediary' particles.* It is possible that intermediary particles exist beyond the framework of the Standard Model, which are immune with respect to interactions with relic radiation and therefore can fly to us from remote sources with energies lying above the GZK limit. Such hypothetical hadrons (the bound states of light gluino and usual quarks) were proposed in paper [27]. Being hadrons, these particles could reproduce the development of EASs [28]. However, this model gives rise to contradictions related to the results of acceleration experiments and the absence of observation of exotic isotopes [28]. The role of an intermediary particle was also ascribed to a hypothetical axion [29–31]. This scenario assumes that high-energy photons oscillate into axions in the magnetic field of a source and, having propagated over cosmological distances without energy loss, oscillate back into photons in the magnetic field of the Galaxy.

● *Violation of the Lorentz invariance.* Threshold energy (1) was obtained assuming the standard Lorentz kinematics. Its violation at high energies could lead to a larger threshold for photomesonic reactions and, therefore, the UHECR spectrum could continue without the GZK flux suppression [32, 33].

3.2 New Telescope Array experiments
The Telescope Array project is a collaboration of several institutions and universities in Japan, the USA, Korea, Russia, and Belgium. From Russia, the Institute for Nuclear Research, RAS participates in the project.

The experimental facility of the Telescope Array (TA) Collaboration is located in the west Utah desert. At present, it is operated with three observation stations using fluorescence detectors (FDs) and arrays of 507 surface detectors (SDs) (Fig. 3), which together form the largest hybrid facility recording UHECRs in the northern hemisphere of Earth. The SDs form an array with a distance of 1.2 km between detectors, which covers an area of 700 km². Three FD stations surrounding the SD array are called Middle Drum (MD), Black Rock Mesa (BR), and Long Ridge (LR). The MD station (Fig. 4) comprises 14 telescopes which were earlier employed in the HiRes experiment. All the equipment at the BR and LR stations was made especially for the TA experiment. Observations with FD stations started in November 2007, and with the surface array in March 2008.

3.2.1 Energy spectrum. By now, the UHECR energy spectra have been obtained by using the TA facility for each of the three data sets: SD data (the SD spectrum), MD station data (which were used to construct the monocular FD spectrum), and hybrid data.

The SD spectrum is constructed using data gathered between May 2004 and February 2010. The exposure is 1500 km² sr per year, which is approximately equal to the total AGASA exposure for the entire observation time. The SD events are reconstructed by fitting the EAS front geometry and the transverse (to the EAS axis) energy density distribution. The number density S_{800} of particles at a distance of 800 m from the EAS axis is utilized to estimate the energy of the initial particle. The relation between S_{800} and energy, as well as the effective aperture are retrieved by the Monte Carlo method. The resulting (preliminary) energy spectrum is presented in Fig. 5.

The obtained SD spectrum was fitted with power functions on the segments. The two break points are found at the values of $\log(E\,[\mathrm{eV}])$ equal to 18.71 and 19.75, which corresponds to the 'ankle' [1] and the onset of the GZK cutoff. For energies exceeding the energy $E = 10^{19.75}$ eV of the break point, five events were recorded, whereas in the case of the continuous power extension of the spectrum, 18.4 events would be expected. Thus, the suppression of the UHECR flux at energies exceeding the GZK limit was found at a confidence level of 3.5σ. The details of the SD analysis are presented in paper [35].

It should be noted that the GZK cutoff was first observed by the FD method in HiRes experiments [36] and was confirmed by the Pierre Auger Observatory [37]. The absence of the GZK cutoff would mean the emergence of new physics which can be manifested differently in various detectors [38]. In this connection, it is important to note that the TA SD detectors are identical to those used in the AGASA facility.

The spectrum obtained at the MD station includes data accumulated for almost three years, from December 2007 to September 2010. The preliminary result is shown in Fig. 5.
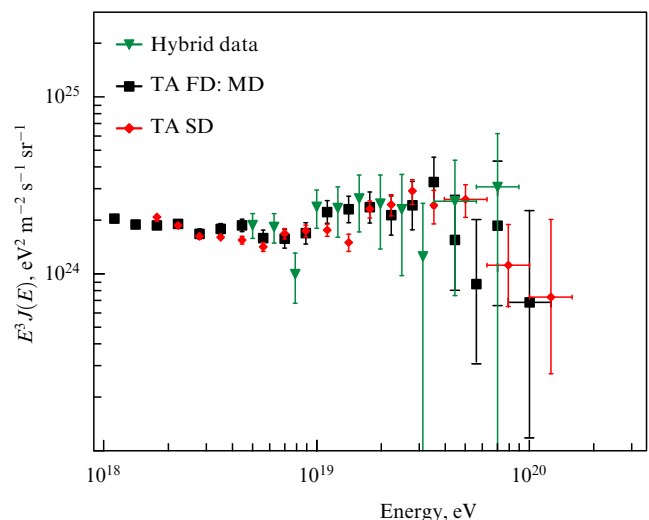

Figure 3. One of the surface detectors in the west Utah desert (USA).

Figure 4. Middle Drum station comprising 14 telescopes recording fluorescent emission of the atmosphere. The long-exposure night shot was contributed by B Stokes.

Figure 5. UHECR spectrum obtained at the Telescope Array Observatory (preliminary results). The spectrum suppression at high energies is statistically meaningful and begins in the GZK energy range.

---

[1] A spectral feature whose position and shape correspond to the theoretically predicted [34] change in the power spectrum, taking into account losses for creation of e^+e^- pairs in the interaction of initial protons with relic radiation.

This TA energy spectrum is consistent with the one obtained in the HiRes experiments [36], and also demonstrates the GZK cutoff. The details of the analysis of these data are presented in the thesis [39].

Hybrid events, i.e., those recorded simultaneously with an SD array and some of the FD stations, have smaller statistics, but nevertheless are preferable for spectral measurements because the energy of the initial particle can be determined calorimetrically using the FD data, while the exposure is accurately determined by means of the SD array. In addition, hybrid events are reconstructed more reliably because more information is available for each event. The preliminary energy spectrum obtained in the hybrid analysis of the TA data accumulated over a year and a half of observations is depicted in Fig. 5; the corresponding details can be found in Ref. [40].

3.2.2 Mass composition.
The longitudinal development of an EAS depends both on the initial particle energy and the particle nature. The atmospheric depth, at which the number of particles in the shower reaches its maximum X_{max}, is a good indicator of the initial particle type. The longitudinal development of the EAS is directly observed by means of fluorescence detectors. Because of this, the FD technique is most convenient for determining the mass (or as the saying is — chemical) composition of UHECRs.

Analyzing EASs by this method, the HiRes Collaboration presented results consistent with the proton-dominated composition of UHECRs in the energy range from 1.6 to 64 EeV (10^{18} eV) [41]. On the other hand, both the average value of X_{max} and the root-mean-square value of its fluctuations, measured at the Pierre Auger Observatory, point to the growing masses of initial particles at energies above 3 EeV, reaching values typical of iron [42].

We are studying the mass composition of UHECRs by measuring X_{max} in a set of the FD stereo data. The analysis presented here is based on the data obtained between November 2007 and September 2010. For events detected simultaneously at two FD stations, the geometry and longitudinal development of the air shower were reconstructed. The energy dependence of the average value of X_{max} obtained in the range from $10^{18.2}$ to 10^{20} eV is plotted in Fig. 6. This figure also shows the Monte Carlo expectation for different models of nuclear interactions. The TA data are in good agreement with the QGSJET-01 prediction for the purely proton composition, and inconsistent with the iron composition for all the interaction models considered. Details of the analysis of the mass composition of UHECRs are presented in Ref. [43].

3.2.3 Constrains on photons.
The suppression of the particle spectrum at the highest energies is not necessarily caused by the GZK effect. It can also be related to an attainment of the acceleration limit by sources, together with the random coincidence of corresponding limiting energies. These alternatives can be distinguished by detecting the photon component of initial particles. The latter appears here as the product of photonuclear reactions. The expected fraction of photons is small, and photons have not yet been observed in UHECRs. The experimental limit of the photon flux for $E > 10$ EeV obtained in TA experiments is [44]

$$F_\gamma < 3.4 \times 10^{-2} \text{ km}^{-2} \text{ sr}^{-1} \text{ year}^{-1} \text{ (95\% CL)}.$$
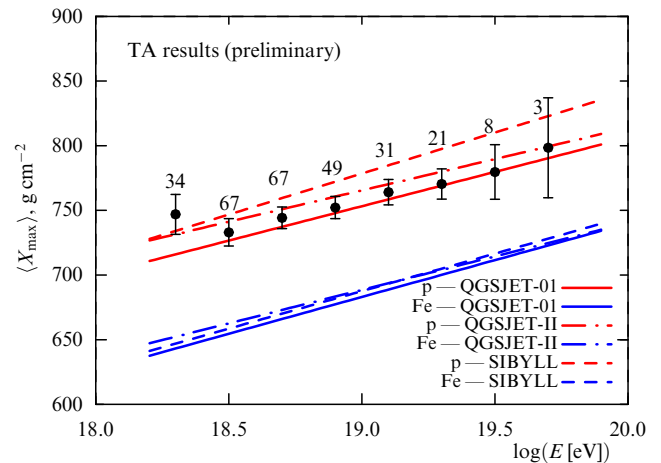
Figure 6. Average value of X_{max} as a function of energy (preliminary TA results). Dots are the FD stereo data (the numbers of recorded events are indicated alongside the dots). The three upper lines correspond to predictions of different interaction models for the purely proton composition: QGSJET-01 (solid line); QGSJET-II (dashed-dot line), and SIBYLL (dashed line). The three lower lines correspond to UHECRs consisting of iron nuclei.

This constrain is the strongest in the northern hemisphere of Earth, exceeding constrains found earlier [45]. The method applied to searching for the photon component was developed in Ref. [46].

3.2.4 Arrival directions.
It may be said without exaggeration that UHECR investigations open a window on the high-energy Universe. The measurement of the arrival direction anisotropy for initial particles is one of the most important scientific issues facing the TA Collaboration. The discovery of such anisotropy will be a key to the identification of UHECR sources, and an important step in the establishment of the chemical composition of UHECRs and measurements of the important parameters of the intergalactic medium, such as the strength and structure of its magnetic fields.

If the discovered suppression of the UHECR spectrum is indeed caused by the GZR effect, then, as discussed in Section 2.1.1, the sources of highest-energy rays should be located inside a sphere 100 Mpc in radius from us. The distribution of matter in the Universe at such spatial scales is strongly inhomogeneous, and therefore the anisotropy of the UHECR flux can be expected. Both variations in the flux at large angular scales and the appearance of point sources on the celestial sphere are expected.

Here, we present the results of correlation analysis [47] of the arrival directions of initial particles with the large-scale structure of the Universe and correlations with active galactic nuclei (AGNs), and also consider autocorrelations on small angular scales. This analysis covers data accumulated for 28 months with a surface detector array, from March 2008 to September 2010. With the cutoff over a zenith angle of 45°, the data set contains 655 events with energies exceeding 10 EeV, 35 events with energies greater than 40 EeV, and 15 events with energies exceeding 57 EeV.

(1) *Autocorrelations.* The arrival directions of initial particles in the AGASA data formed clusters (doublets and triplets) with an angular size of 2.5° [48, 49]. These results can be treated as the formulation of the statistical hypothesis according to which the arrival directions are anisotropic. Here, we will verify this hypothesis by utilizing TA data. By
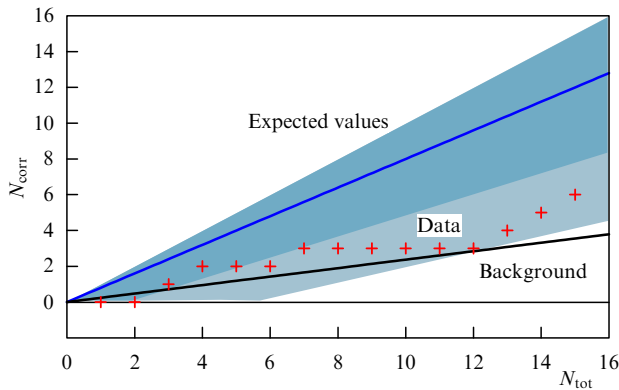
Figure 7. Result of a correlation test with AGNs. On the abscissa, the number of recorded events with $E > 57$ EeV is plotted in chronological order; on the ordinate is the number of correlating events. According to the Auger hypothesis, the expectation is shown by the line surrounded by confidence intervals 1σ and 2σ. The lower thick line is the expectation for the isotropic distribution. Crosses mark TA data.

following the AGASA analysis, we will use the energy cutoffs $E > 10$ EeV and $E > 40$ EeV in the data set. Then, all the events are counted in which arrival directions form pairs with the angular distance smaller than $2.5°$. The number obtained is compared with that expected for the isotropic distribution of arrival directions. In a data set with $E > 10$ EeV, we found 311 such pairs, whereas 323 pairs are expected for the isotropic distribution. A set with $E > 40$ EeV contains one pair, whereas the expected value is 0.838. Thus, data redundancy is absent. Then, we weakened the formulation of the hypothesis and performed such a test at all angular scales from 0 to $30°$ and again obtained a negative result. Thus, no anisotropy of the TA data was observed at small angular scales.

(2) *Correlations with active galaxies.* The Pierre Auger Observatory reported correlations [50] of UHECRs with energies exceeding 57 EeV with near (a distance of less than 75 Mpc) AGNs. Correlations were observed at angular scales of 3.1%. In a control data set consisting of 13 events, 9 events correlated, which amounts to 69%. Here, we will verify the corresponding statistical hypothesis.

The TA exposure, unlike the Auger Observatory exposure, is concentrated in the northern celestial hemisphere, where the catalogue [51] used for analysis contains many AGNs, and therefore a greater fraction of correlating events can be expected. Assuming that the luminosities of AGNs in UHECRs are the same, we estimate this fraction as 73% for the TA observation. The result of the corresponding correlation analysis is given in Fig. 7. So far no certain conclusions can be made because the available statistics are very scarce, making the TA data consistent with both the isotropic distribution and the AGN hypothesis.

(3) *Correlation with the structure.* In this case, we verify the hypothesis that TA events occur in sources which follow the distribution of matter in the Universe. Such a correlation should inevitably exist if initial particles are protons and the intergalactic magnetic fields are not too strong. We perform our analysis by the method developed in Ref. [52] and used earlier to analyze the HiRes data [53]. In this method, first the expected distribution of the UHECR flux in the sky is calculated, assuming that sources follow the distribution of visible matter. Then, the expected distribution of sources is compared with real data.

Correlation with the large-scale structure of the Universe was verified for energies $E > 40$ EeV and $E > 57$ EeV. Both data sets were found to be consistent with this hypothesis. The data set with $E > 40$ EeV is also in agreement with the isotropic distribution, whereas the data set with $E > 57$ EeV is inconsistent with the isotropic distribution at a confidence level of 95%. To distinguish reliably these two hypotheses, statistics exceeding in number the existing ones by several times is required.

4. Conclusion

The Telescope Array is the largest observatory in the northern hemisphere of Earth for studying ultrahigh-energy cosmic rays. The TA detectors began to operate in March 2008. The spectrum of cosmic rays has been measured, and the GZK cutoff has been found at energies exceeding $10^{19.75}$ eV at a confidence level of 3.5σ. The mass composition in the energy range from $10^{18.2}$ to 10^{20} eV is consistent with the purely proton one. The arrival direction distribution for initial particles is still consistent with the isotropic distribution of their sources.

References

1. Greisen K *Phys. Rev. Lett.* **16** 748 (1966)
2. Zatsepin G T, Kuz'min V A *Pis'ma Zh. Eksp. Teor. Fiz.* **4** 114 (1966) [*JETP Lett.* **4** 78 (1966)]
3. Tinyakov P G, Tkachev I I *Astropart. Phys.* **24** 32 (2005); astro-ph/0411669
4. Neronov A, Semikoz D V *Phys. Rev. D* **80** 123012 (2009); arXiv:0910.1920
5. Dolag K, Grasso D, Springel V, Tkachev I *Pis'ma Zh. Eksp. Teor. Fiz.* **79** 719 (2004) [*JETP Lett.* **79** 583 (2004); astro-ph/0310902
6. Neronov A, Vovk I *Science* **328** 73 (2010); arXiv:1006.3504
7. Linsley J *Phys. Rev. Lett.* **10** 146 (1963)
8. Winn M M et al. *J. Phys. G Nucl. Phys.* **12** 653 (1986)
9. Lawrence M A, Reid R J O, Watson A A *J. Phys. G Nucl. Part. Phys.* **17** 733 (1991)
10. Afanasiev B N et al., in *Proc. Intern. Symp. on Extremely High Energy Cosmic Rays: Astrophysics and Future Observatories* (Ed. M Nagano) (Tokyo: Univ. of Tokyo, 1996) p. 32
11. Antonov E E et al. *Pis'ma Zh. Eksp. Teor. Fiz.* **69** 614 (1999) [*JETP Lett.* **69** 650 (1999)]
12. Takeda M et al. *Phys. Rev. Lett.* **81** 1163 (1998)
13. Hayashida N et al., astro-ph/0008102
14. Bird D J et al. *Astrophys. J.* **441** 144 (1995)
15. Jui C H et al., in *Proc. 27th Intern. Conf. on Cosmic Rays: ICRC 2001, Hamburg* Vol. 1 (Göttingen: Copernicus Gessellschaft, 2001) p. 354

16. Mantsch P (for the Pierre Auger Collab.) "The Pierre Auger Observatory progress and first results", astro-ph/0604114

17. Tokuno H et al. *AIP Conf. Proc.* **1238** 365 (2010)

18. Boldt E, Ghosh P *Mon. Not. R. Astron. Soc.* **307** 491 (1999); astro-ph/9902342

19. Neronov A, Tinyakov P, Tkachev I *Zh. Eksp. Teor. Fiz.* **127** 744 (2005) [*JETP* **100** 656 (2005)]; astro-ph/0402132

20. Berezinsky V, Kachelrieß M, Vilenkin A *Phys. Rev. Lett.* **79** 4302 (1997); astro-ph/9708217

21. Kuzmin V A, Rubakov V A *Yad. Fiz.* **61** 1122 (1998) [*Phys. At. Nucl.* **61** 1028 (1998); astro-ph/9709187

22. Chung D J H, Kolb E W, Riotto A *Phys. Rev. D* **59** 023501 (1999)

23. Kuzmin V A, Tkachev I I *Pis'ma Zh. Eksp. Teor. Fiz.* **68** 255 (2005) [*JETP Lett.* **68** 271 (1998)]

24. Kuzmin V, Tkachev I *Phys. Rev. D* **59** 123006 (1999)

25. Dubovsky S L, Tinyakov P G *Pis'ma Zh. Eksp. Teor. Fiz.* **68** 99 (1998) [*JETP Lett.* **68** 107 (1998); hep-ph/9802382

26. Berezinsky V, Mikhailov A A *Phys. Lett. B* **449** 237 (1999); astro-ph/9810277

27. Chung D J H, Farrar G R, Kolb E W *Phys. Rev. D* **57** 4606 (1998); astro-ph/9707036

28. Berezinsky V, Kachelrieß M, Ostapchenko S *Phys. Rev. D* **65** 083004 (2002); astro-ph/0109026

29. Gorbunov D S, Raffelt G G, Semikoz D V *Phys. Rev. D* **64** 096005 (2001); hep-ph/0103175

30. Csáki C et al. *JCAP* (05) 005 (2003); hep-ph/0302030

31. Fairbairn M, Rashba T, Troitsky S V, arXiv:0901.4085

32. Coleman S, Glashow S L *Phys. Rev. D* **59** 116008 (1999); hep-ph/9812418

33. Dubovsky S L, Tinyakov P G *Astropart. Phys.* **18** 89 (2002); astro-ph/0106472

34. Berezinsky V, Gazizov A Z, Grigorieva S I *Phys. Lett. B* **612** 147 (2005); astro-ph/0502550

35. Stokes B et al. (for the Telescope Array Collab.), in *Proc. of the Intern. Symp. on the Recent Progress of Ultra-High Energy Cosmic Ray Observation*: *UHECR, Nagoya, Japan, December 10–12, 2010*

36. Abbasi R U et al. (HiRes Collab.) *Phys. Rev. Lett.* **100** 101101 (2008); astro-ph/0703099

37. Abraham J et al. (Pierre Auger Collab.) *Phys. Rev. Lett.* **101** 061101 (2008); arXiv:0806.4302

38. Kalashev O E, Rubtsov G I, Troitsky S V *Phys. Rev. D* **80** 103006 (2009); arXiv:0812.1020

39. Rodriguez D C, Ph.D. Thesis (Salt Lake City, UT: Univ. of Utah, 2011)

40. Ikeda D et al. (for the Telescope Array Collab.), in *Proc. of the Intern. Symp. on the Recent Progress of Ultra-High Energy Cosmic Ray Observation*: *UHECR, Nagoya, Japan, December 10–12, 2010*

41. Abbasi R U et al. (HiRes Collab.) *Phys. Rev. Lett.* **104** 161101 (2010); arXiv:0910.4184

42. Abraham J et al. (Pierre Auger Collab.) *Phys. Rev. Lett.* **104** 091101 (2010); arXiv:1002.0699

43. Tameda Y et al. (for the Telescope Array Collab.), in *Proc. of the Intern. Symp. on the Recent Progress of Ultra-High Energy Cosmic Ray Observation*: *UHECR, Nagoya, Japan, December 10–12, 2010*

44. Rubtsov G I et al. (for the Telescope Array Collab.), in *Proc. of the Intern. Symp. on the Recent Progress of Ultra-High Energy Cosmic Ray Observation*: *UHECR, Nagoya, Japan, December 10–12, 2010*

45. Glushkov A V et al. *Pis'ma Zh. Eksp. Teor. Fiz.* **85** 163 (2007) [*JETP Lett.* **85** 131 (2007)]; astro-ph/0701245

46. Gorbunov D S, Rubtsov G I, Troitsky S V *Astropart. Phys.* **28** 28 (2007); astro-ph/0606442

47. Tinyakov P et al. (for the Telescope Array Collab.), in *Proc. of the Intern. Symp. on the Recent Progress of Ultra-High Energy Cosmic Ray Observation*: *UHECR, Nagoya, Japan, December 10–12, 2010*

48. Hayashida N et al. *Phys. Rev. Lett.* **77** 1000 (1996)

49. Tinyakov P G, Tkachev I I *Pis'ma Zh. Eksp. Teor. Fiz.* **74** 3 (2001) [*JETP Lett.* **74** 1 (2001)]; astro-ph/0102101

50. Abraham J et al. (Pierre Auger Collab.) *Science* **318** 938 (2007); arXiv:0711.2256

51. Veron-Cetty M P, Veron P "Quasars and active galactic nuclei", ESO Scientific Report 19, 9th ed. (2000)

52. Koers H B J, Tinyakov P *JCAP* (04) 003 (2009); arXiv:0812.0860

53. Abbasi R U et al., arXiv:1002.1444

T2K neutrino experiment: first results

Yu G Kudenko

1. Introduction

The discovery of neutrino oscillations became direct experimental evidence of the existence of new physics beyond the framework of the Standard Model and simultaneously marked the beginning of the study of this physics. As follows from the oscillations, neutrinos possess a small nonzero mass, they mix, and neutrino flavors (lepton numbers) are not conserved. Neutrino oscillations are described by the so-called neutrino Standard Model (νSM), which is the minimal model describing the mixing of three neutrino types. The physics of neutrino oscillations is described by a unitary matrix U [1] that relates three types of active neutrinos with left-handed helicity, ν_e, ν_μ, and ν_τ, to the mass eigenstates ν_1, ν_2, and ν_3 with the respective masses m_1, m_2, and m_3. In a form convenient for physical analysis, the matrix U can be represented as follows:

$$U = \begin{pmatrix} 1 & 0 & 0 \\ 0 & c_{23} & s_{23} \\ 0 & -s_{23} & c_{23} \end{pmatrix} \begin{pmatrix} c_{13} & 0 & s_{13}\exp(-i\delta) \\ 0 & 1 & 0 \\ -s_{13}\exp(i\delta) & 0 & c_{13} \end{pmatrix}$$
$$\times \begin{pmatrix} c_{12} & s_{12} & 0 \\ -s_{12} & c_{12} & 0 \\ 0 & 0 & 1 \end{pmatrix}. \tag{1}$$

In this expression, $s_{ij} \equiv \sin\theta_{ij}$ and $c_{ij} \equiv \cos\theta_{ij}$ ($i, j = 1, 2, 3$). Neutrino oscillations are described by six parameters: two independent mass squared differences: $\Delta m_{12}^2 = m_2^2 - m_1^2$ and $\Delta m_{23}^2 = m_3^2 - m_2^2$; three mixing angles: θ_{12}, θ_{23}, θ_{13}, and a CP-odd phase δ.

Experiments with atmospheric [2], solar [3–8], reactor [9], and accelerator [10, 11] neutrinos measured four parameters θ_{12}, θ_{23}, Δm_{12}^2, and Δm_{23}^2: $\tan^2\theta_{12} = 0.47^{+0.06}_{-0.05}$, $\Delta m_{12}^2 = 7.59^{+0.21}_{-0.21} \times 10^{-5}$ eV^2, $\sin^2 2\theta_{23} > 0.92$ for a 90-percent confidence interval (90% CL), and $\Delta m_{23}^2 = (2.43 \pm 0.13) \times 10^{-3}$ eV^2. It is pertinent to note that the sign of Δm_{23}^2 is unknown, i.e., the neutrino mass hierarchy has not been determined. Both the normal hierarchy, $m_3 \gg m_2 > m_1$, and inverse hierarchy, $m_2 > m_1 \gg m_3$, are possible. Furthermore, the parameters θ_{13} and δ have not been measured. The best limit, $\sin^2 2\theta_{13} < 0.15$ (90% CL) for $\Delta m_{23}^2 = 2.43 \times 10^{-3}$ eV^2, was obtained in the ChOOZ experiment [12].

Since $|\Delta m_{12}^2| \ll |\Delta m_{13}^2| \simeq |\Delta m_{23}^2|$ and the typical baselines of accelerator experiments for studying neutrino oscillations in the region of 'atmospheric' parameters ($\Delta m_{23}^2 \sim (2-3) \times 10^{-3}$ eV^2) amount to several hundred kilometers, the contribution of Δm_{12}^2-bearing terms to the oscillation probability is small, so that approximate expressions for muon neutrino

Yu G Kudenko Institute for Nuclear Research,
Russian Academy of Sciences, Moscow, Russian Federation
E-mail: kudenko@inr.ru